Continuous-Time Monitoring of Landau-Zener Interference in a Cooper-Pair Box

Mika Sillanpää,[1] Teijo Lehtinen,[1] Antti Paila,[1] Yuriy Makhlin,[2,1] and Pertti Hakonen[1]

[1]*Low Temperature Laboratory, Helsinki University of Technology, FIN-02015 HUT, Finland*
[2]*Landau Institute for Theoretical Physics, 119334 Moscow, Russia*

Landau-Zener (LZ) tunneling can occur with a certain probability when crossing energy levels of a quantum two-level system are swept across the minimum energy separation. Here we present experimental evidence of quantum interference effects in solid-state LZ tunneling. We used a Cooper-pair box qubit where the LZ tunneling occurs at the charge degeneracy. By employing a weak nondemolition monitoring, we observe interference between consecutive LZ-tunneling events; we find that the average level occupancies depend on the dynamical phase. The system's unusually strong linear response is explained by interband relaxation. Our interferometer can be used as a high-resolution Mach-Zehnder–type detector for phase and charge.

PACS numbers: 74.50.+r, 73.23.Hk

The Landau-Zener (LZ) tunneling is a celebrated quantum-mechanical phenomenon, taking place at the intersection of two energy levels that repel each other [1]. The LZ theory, developed in the early 1930s in the context of slow atomic collisions [2–4] and spin dynamics [5], demonstrated that transitions are possible between two approaching levels as a control parameter is swept across the point of minimum energy splitting. The asymptotic probability of a LZ-tunneling transition is given by [2–5]

$$P_{LZ} = \exp\left(-2\pi \frac{\Delta^2}{\hbar v}\right), \quad (1)$$

where $v \equiv d(\varepsilon_1 - \varepsilon_0)/dt$ denotes the variation rate of the energy spacing for noninteracting levels, and 2Δ is the minimum energy gap.

Yet for truly quantum-mechanical systems, more fundamental is the transition *amplitude*, which allows for interference. As two atoms collide, the wave-function phase accumulated between the incoming and outgoing traversals varies with, e.g., the collision energy giving rise to Stueckelberg oscillations in the populations [6]. Typically, however, the phase is large and rapidly varies with energy, which allows one to average over these fast oscillations [4,7], neglecting the interference.

Recently, quantum coherence in mesoscopic Josephson tunnel junctions has been investigated extensively [8–11]. In these artificial two-level systems, energy scales can easily be tuned into a range feasible for studies of fundamental phenomena. We used a charge qubit based on a Cooper-pair box (CPB) to obtain the first evidence of quantum interference associated with Landau-Zener tunneling in nonatomic systems. A continuous nondemolition measurement developed by us [12], which provides minimal backaction to the qubit, allowed for monitoring the average level occupancies of the CPB and thus observation of the LZ interference.

Our CPB is a single-Cooper-pair transistor (SCPT) embedded into a superconducting loop. The island has the charging energy $E_C = e^2/(2C) \sim 1$ K, and the junctions

have the Josephson energies $E_J(1 \pm d)$, where d quantifies the asymmetry. The SCPT is equivalent to a CPB, but with a Josephson energy of $2E_J \cos(\phi/2)$ tunable by the superconducting phase across the two junctions, $\phi = 2\pi\Phi/\Phi_0$. When $E_C \gg E_J$, the Hamiltonian of the CPB is conveniently written in the eigenbasis $\{|2ne\rangle\}$ of the island charge operator, taking only two charge states into account:

$$H = -\frac{1}{2}B_z\sigma_z - \frac{1}{2}B_x\sigma_x = \begin{pmatrix} \epsilon(n_g) & -\Delta \\ -\Delta & -\epsilon(n_g) \end{pmatrix}, \quad (2)$$

where $\epsilon = -\frac{1}{2}B_z = -2E_C(1 - n_g)$ and $\Delta = \frac{1}{2}B_x = E_J\cos(\phi/2)$. The asymmetry $d \neq 0$ in Josephson energies would limit the minimum off-diagonal coupling $|\Delta|$. The eigenvalues of Eq. (2), $E_0(n_g, \phi)$ and $E_1(n_g, \phi)$, are the two lowest bands as illustrated by Fig. 1(a). By $|0\rangle = [1, 0]^T$ and $|1\rangle = [0, 1]^T$, we denote the corresponding (n_g, ϕ)-dependent eigenfunctions. Far from the crossing, they are roughly charge eigenstates.

The Hamiltonian of Eq. (2) is similar to the original LZ problem, and the linearly growing band gap $E_1 - E_0 \approx \varepsilon_1 - \varepsilon_0 = 4E_C(1 - n_g)$ has the minimum 2Δ at the charge degeneracy (avoided crossing) at $n_g = 1$. As n_g is swept through this point (similar to the interatomic distance during a collision), one obtains the asymptotic transition probability between levels 0 and 1 as in Eq. (1). This kind of incoherent limit of the LZ problem has also been observed in superconducting qubits [10].

More fundamentally, however, the asymptotic probability in Eq. (1) comes from the unitary transformation taking place at the avoided crossing [13,14]:

$$U_1 = \begin{pmatrix} \cos(\theta/2)\exp(i\tilde{\phi}_S) & i\sin(\theta/2) \\ i\sin(\theta/2) & \cos(\theta/2)\exp(-i\tilde{\phi}_S) \end{pmatrix}. \quad (3)$$

Here, $\sin^2(\theta/2) = P_{LZ}$. The phase jump $\tilde{\phi}_S = \phi_S - \pi/2$ is due to the Stokes phase ϕ_S related to the general Stokes phenomenon [15]. It depends on the adiabaticity parameter $\delta = \Delta^2/\hbar v$ [cf. Eq. (1)], viz., $\phi_S = \pi/4 + \arg[\Gamma(1 - i\delta)] + \delta(\ln\delta - 1)$, where Γ is the Gamma function. In
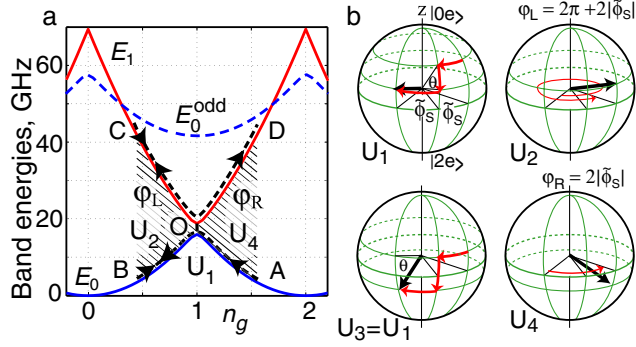
FIG. 1 (color online). Landau-Zener interference in a CPB. (a) The energy diagram: As n_g is modulated, the CPB evolves from the initial state A through the avoided crossing O ($n_g = 1$) towards B (no LZ tunneling) or C (with LZ tunneling). On the return journey, the final state D is reached by remaining on the excited band (from C) or by LZ tunneling (from B). The dynamical phases $\varphi_{L,R}$ are accumulated between O and the turning points. The uppermost dashed line represents the odd parity state E_0^{odd}. (b) Interpretation of one cycle of LZ interference as four spin rotations on the Bloch sphere, with one possible set of $\varphi_{L,R}$ yielding constructive interference (see text). The black arrows indicate the final position of the Bloch vector after each step. Number states of the island charge $|2ne\rangle$ are aligned along the z axis.

the adiabatic limit $\phi_S \rightarrow 0$, and in the sudden limit $\phi_S = \pi/4$. On the Bloch sphere, a single LZ event [Eq. (3)] is seen as a combination of x and z rotations [U_1 and U_3 in Fig. 1(b)].

The natural manner to look for quantum coherence in LZ tunneling is to repeat the level crossing faster than the relevant time scales, as suggested by Shytov *et al.* [16]. Indeed, subsequent LZ-tunneling events with time interval τ_p can interfere, provided phase coherence is preserved and these events do not overlap [13,14], $\tau_z < \tau_p < \tau_{\text{coh}}$. Here, the time of an LZ-tunneling event [17] is $\tau_z \sim \sqrt{\hbar/v} \max(1, \sqrt{\Delta^2/\hbar v})$. In charge qubits, it is easy to make $\tau_z \ll \tau_{\text{coh}}$, where the coherence time is $\tau_{\text{coh}} = \min(T_1, T_2)$ with T_1 and T_2 corresponding to the relaxation and dephasing time, respectively. For example, $\Delta = 2$ GHz and $v = 40$ GHz per 1 ns give $\tau_z \sim 0.1$ ns, which is well within experimental reach.

To generate the required conditions, we used a strong gate charge sweep $n_g(t) = n_{g0} + \delta n_{\text{rf}} \sin(\omega_{\text{rf}} t)$, in general offset from the crossing point. One cycle takes the CPB twice through the crossing and involves two dynamical phase shifts φ_L and φ_R, on the left and right sides:

$$\varphi = -\frac{1}{\hbar} \int [E_1(n_g(t)) - E_0(n_g(t))] dt. \quad (4)$$

During a single drive cycle, the state vector evolves according to the transformation $U = U_4 U_3 U_2 U_1$, which is illustrated in Fig. 1(b) as successive spin rotations (σ are the Pauli matrices, and $U_3 = U_1$):

$$U = \exp(-i\tfrac{1}{2}\varphi_R \sigma_z) U_1 \exp(-i\tfrac{1}{2}\varphi_L \sigma_z) U_1. \quad (5)$$

The transition amplitude $p_{\text{AD}} = \langle \Psi | 1 \rangle = \langle 0 | U^\dagger | 1 \rangle$ is the z projection of the Bloch vector. Evaluating Eq. (5) we find $p_{\text{AD}} = i \exp(i\varphi_R/2) \cos(\varphi_L/2 - \tilde{\phi}_S) \sin(\theta)$, and the probability $P_{\text{AD}} = |p_{\text{AD}}|^2$ of reaching the point D:

$$|p_{\text{AD}}|^2 = 2P_{\text{LZ}}(1 - P_{\text{LZ}})[1 + \cos(\varphi_L - 2\tilde{\phi}_S)]. \quad (6)$$

It is easy to see in Fig. 1(b) that P_{AD} is generally maximized (constructive interference) when the z rotations bring the Bloch vector back to the starting meridian, for then the total x rotation is maximized. This is achieved when the total phase $\varphi_L - 2\tilde{\phi}_S$ is a multiple of 2π. Under continuous driving, this has the obvious generalization which corresponds to the Bloch vector rotating stepwise around a fixed axis in the x-y plane; the condition

$$\varphi_{L,R} - 2\tilde{\phi}_S \text{ are multiples of } 2\pi \quad (7)$$

ensures constructive interference (50% time-averaged populations of both levels). For example, in the adiabatic limit, $\varphi_{L,R}$ have to be odd multiples of π. The resonance conditions in Eq. (7) are seen overlaid in Fig. 3 (see below) as the black solid and dashed lines.

Our experimental scheme is illustrated in Fig. 2. The weak, continuous measurement signal tracks the time average, subject to a strong LZ drive, of the Josephson capacitance of a CPB: $C_{\text{eff}} \propto \frac{\partial^2 E(\phi, n_g)}{\partial n_g^2}$, probed at $f_0 = 803$ MHz. The scheme is discussed in detail in Ref. [12]. The difference in C_{eff} for the levels 0, 1 allows us to determine the average state of the CPB (see the discussion below).

We made extensive scans of the CPB reflection by varying the LZ-drive frequency $f_{\text{rf}} = 0.1$–20 GHz and its amplitude $\delta n_{\text{rf}} = 0$–3 electrons, as well as the qubit bias n_{g0} and ϕ. We observe a clear interference pattern (Fig. 3) whose main features confirm the coherent LZ-tunneling picture: (1) onset of the interference speckles where the rf drive just reaches the avoided crossing, with
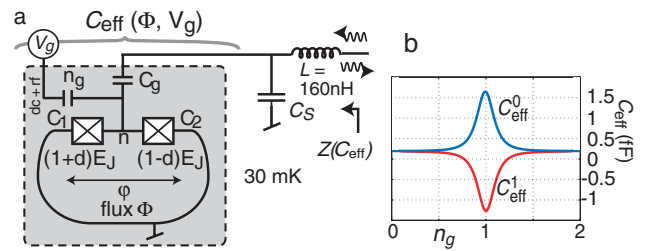

FIG. 2 (color online). Schematics of our experiment. (a) The resonant frequency $f_0 \sim 800$ MHz of the lumped-element LC circuit is tuned by the Josephson capacitance C_{eff} of the CPB shown in the scanning electron micrograph. The maximum CPB Josephson energy $2E_J = 12.5$ GHz could be tuned down to 2.7 GHz by magnetic flux Φ. The total junction capacitance amounts to $C_J = C_1 + C_2 \sim 0.44$ fF, yielding a Coulomb energy of $e^2/2(C_J + C_g) = 1.1$ K. (b) C_{eff} calculated for the two lowest levels of our CPB with $E_J/E_C = 0.27$ and asymmetry $d = 0.22$, at $\phi = 0$.
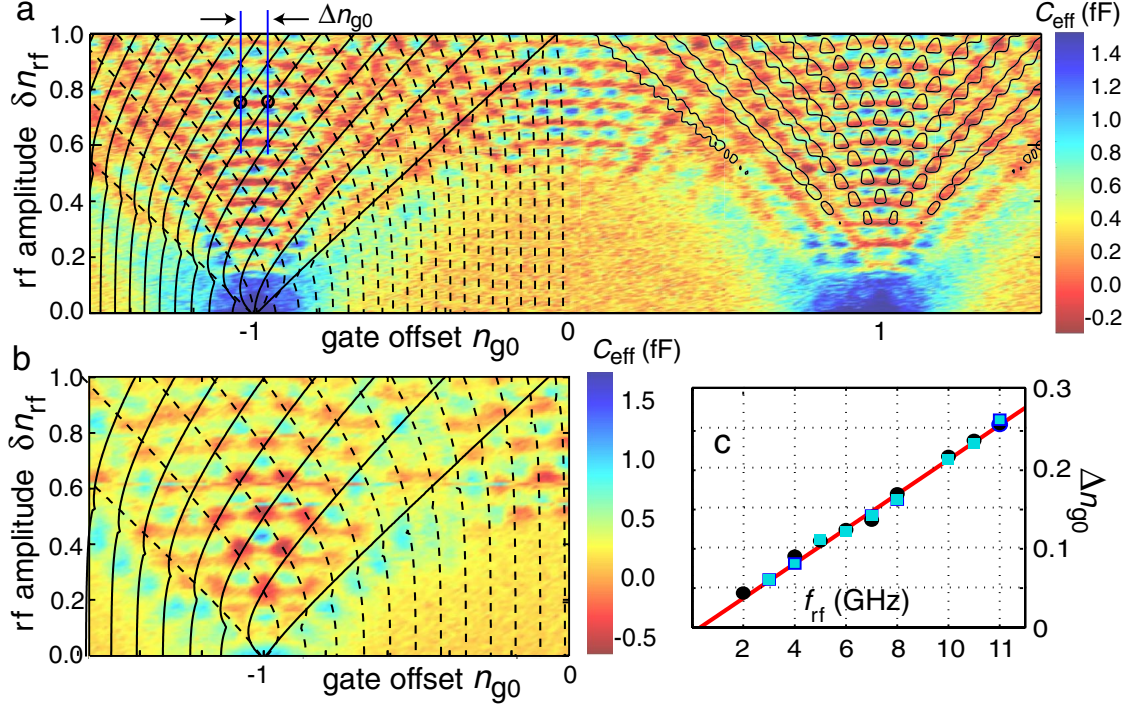
FIG. 3 (color online).   Interference patterns, measured via the microwave phase shift. (a) $f_{rf} = 4$ GHz and phase $\phi = 0$ (i.e., level repulsion $2\Delta = 2E_J = 12.5$ GHz). The color codes indicate the equivalent capacitance obtained using standard circuit formulas. Around $n_{g0} = -1$, the conditions of constructive Landau-Zener interference are illustrated: $\varphi_L - 2\tilde{\phi}_S$ (solid lines) and $\varphi_R - 2\tilde{\phi}_S$ (dashed line) are multiples of 2π [see Eq. (7)], with the v-dependent Stokes phase ϕ_S. The highest (red) population of the upper state is expected when both conditions are satisfied. The equicapacitance contour $C_{eff} = 0$ around $n_g = 1$, obtained from the simulation of the Bloch equations (Fig. 4), agrees well with the predicted resonance grid and with the data. (b) The corresponding measurement with $f_{rf} = 7$ GHz. (c) The average gate spacing between the central interference peaks [see (a)], for the phase bias 0 (square) and π (circle). The expected linear behavior yields a fit $E_C = 1.1$, about 25% higher than we obtained by rf spectroscopy [12].

a linear dependence between n_{g0} and the rf amplitude; (2) the density of the dots is proportional to $1/f_{rf}$ in the direction of n_{g0} as well as δn_{rf}; (3) the pattern loses its contrast below a certain drive frequency, here at $f_{rf} \sim$ 2 GHz, due to the loss of phase memory over a single LZ cycle. Note also the destructive interference dots at high drives, where the qubit remains basically on the lowest level, thus vindicating the "coherent destruction of tunneling" [18].

We attribute the slight asymmetries in the data with respect to $n_g = \pm 1$ to background charge drift caused by the strong rf drive. The theory grids in Figs. 3(a) and 3(b) were calculated by the v-dependent Stokes phase ϕ_S. However, since the Stokes phase amounts typically only to a 10%–20% shift of the grid, roughnesses in the data do not allow a clear verification of such a small effect.

The patterns are $2e$ periodic in n_{g0} at weak rf excitation. At stronger excitation on the order of $e/2$, an additional, shifted pattern makes the signal almost e periodic [Fig. 3(a)]. The origin of these odd sectors can be understood from the energy diagram in Fig. 1: When the rf drive brings the system past a crossing point of E_1 and E_0^{odd}, it becomes energetically favorable to enter an odd particle-number state [19], resulting in a shift by e in the interference pattern.

According to Eq. (7), the phase difference $\varphi_- \equiv \varphi_L - \varphi_R \simeq 2\pi \frac{4E_C(n_{g0}-1)}{\hbar\omega_{rf}}$ is a multiple of 2π at resonances, implying the location of the population peaks on the lines of fixed rf amplitude with spacings $\Delta n_{g0} = \hbar\omega_{rf}/(2E_C)$. We observe the expected linear frequency dependence, as illustrated in Fig. 3(c).

The magnitude of the response in Fig. 3 forces one to study a complicated relation between the relevant time scales. $C_{eff}(n_{g0})$ generally has contributions from how both the energies and populations depend on n_g. Furthermore, one has to time average over the strong LZ swing in $n_g(t)$. Therefore, we have

$$C_{eff}(n_{g0}) \propto \left\langle \frac{d^2}{dn_g^2} [p_0(n_g)E_0(n_g) + p_1(n_g)E_1(n_g)] \right\rangle. \quad (8)$$

The dominant contribution is determined by the relative magnitude of the time scales of the LZ drive $1/f_{rf}$, time of the measurement swing $1/f_0$, and the relaxation time T_1 (we suppose $f_{rf} \gg f_0$). (a) Long relaxation time, $T_1 \gg 1/f_0$. During the measurement swing, populations do not relax into their quasiequilibrium values, $d^2/dn_g^2(p_{0,1}(n_g)) = 0$ and C_{eff} is small. (b) A short relaxation time, $T_1 \ll 1/f_0$. The populations follow $p_{0,1}(n_g)$ according to the instantaneous ac gate charge due to the
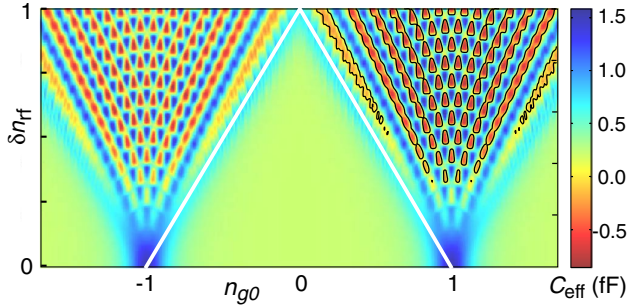
FIG. 4 (color online). Calculated C_{eff}, using Bloch equations and linear-response theory, with $\alpha = 0.04$, $\delta n_{ac} = 0.06e$ pp. The inclined white lines indicate the threshold of the LZ tunneling, where the driving signal $n_g(t)$ touches, but does not cross, a degeneracy point. The comparison with data in Fig. 3 is performed by the equicapacitance contours for $C_{eff} = 0$ fF.

measurement swing, and Eq. (8) gives a large C_{eff}. (c) Intermediate case. This corresponds to our experiment, where $T_1 \sim 5$ ns $\sim f_0 \sim 1$ ns. The value of C_{eff} is between (a) and (b). Therefore, we have a somewhat unexpected result that the magnitude of the measured response can be *increased* by relaxation.

To begin with, we numerically solved the Bloch equations [20,21]. We assumed that the T_1 and T_2 relaxation times are dominated by charge noise, modeled by an Ohmic bath with the strength $\alpha = (1 + [C_1 + C_2]/C_g)^{-2} \frac{2e^2}{h} R$, where R is the effective impedance of the gate voltage circuit. For our sample, $\alpha \sim 10^{-2}$ due to strong coupling to the environment via the gate. Various descriptions of dissipation are expected to yield the same result: one can show that in the description of crossing a narrow degeneracy region, dissipation can be effectively described by a few constants (cf. Ref. [16]).

In order to properly include the interplay between the time scales as described above, we used the linear-response theory to extract C_{eff}, with a weak measurement ac signal on, of amplitude $\delta n_{ac} = C_g \delta V_{ac}$. We calculate the time-dependent expectation value for the charge Q_g on C_g, viz., $\langle Q_g \rangle(t) = \text{Tr}(\rho * Q_g)$, where $Q_g = C_g(\delta V_{ac} - dE/e dn_g)$, and the density matrix is expressed in the energy eigenbasis. From $\langle Q_g \rangle(t)$ we pick up its quadrature components, $Q_{\omega_{in}}$ and $Q_{\omega_{out}}$, at the measurement frequency. The presence of the small resistive component $Q_{\omega_{out}}$ is equivalent to having dissipation. By modeling the input impedance as C_{eff} in series with a small resistor, we find from the imaginary part $C_{eff} = \frac{Q_{\omega_{in}}^2 + Q_{\omega_{out}}^2}{Q_{\omega_{in}} \delta V_{ac}}$. The resulting capacitance at $f_{rf} = 4$ GHz is illustrated in Fig. 4. The values $\alpha = 0.04$ and $\delta n_{ac} = 0.03$ were taken in order to match the measured pattern. This corresponds at the degeneracy point to $T_2 \sim 0.5$ ns which is close to other estimates. The calculation is seen to reproduce the major features of the measured interferograms [22].

The LZ interference in Fig. 1(a) can also be interpreted as two partial waves, *AOBOD* and *AOCOD*, similarly to an

optical Mach-Zehnder interferometer [23]. We propose to apply the LZ interferometry for sensitive detection of phase and charge [12,24–26], where it can be viewed as integrating phase amplifier for the superconductor phase ϕ across the device. The interferometer transforms tiny changes of ϕ (or magnetic flux Φ) into a huge modulation of the wave-function phase φ by basically integrating the hatched area [11] in Fig. 1, but with a limitation on the measurement signal amplitude.

[1] J. von Neumann and E. Wigner, Phys. Z. **30**, 467 (1929).
[2] L. Landau, Phys. Z. Sowjetunion **2**, 46 (1932).
[3] C. Zener, Proc. R. Soc. A **137**, 696 (1932).
[4] E. C. G. Stueckelberg, Helv. Phys. Acta **5**, 369 (1932).
[5] E. Majorana, Nuovo Cimento **9**, 43 (1932).
[6] D. Coey, D. C. Lorents, and F. T. Smith, Phys. Rev. **187**, 201 (1969).
[7] L. Landau, Phys. Z. Sowjetunion **1**, 88 (1932).
[8] Y. Nakamura, Yu. A. Pashkin, and J. S. Tsai, Nature (London) **398**, 786 (1999).
[9] Yu. Makhlin, G. Schön, and A. Shnirman, Rev. Mod. Phys. **73**, 357 (2001).
[10] A. Izmalkov *et al.*, Europhys. Lett. **65**, 844 (2004).
[11] L. Y. Gorelik *et al.*, Phys. Rev. Lett. **81**, 2538 (1998).
[12] M. A. Sillanpää *et al.*, Phys. Rev. Lett. **95**, 206806 (2005).
[13] E. Shimshoni and Y. Gefen, Ann. Phys. (N.Y.) **210**, 16 (1991).
[14] Y. Kayanuma, Phys. Rev. A **55**, R2495 (1997).
[15] M. V. Berry, in *Asymptotics Beyond All Orders*, edited by H. Segur and S. Tanveer (Plenum, New York, 1991), p. 1.
[16] A. V. Shytov, D. A. Ivanov, and M. V. Feigel'man, Eur. Phys. J. B **36**, 263 (2003).
[17] K. Mullen *et al.*, Phys. Rev. Lett. **62**, 2543 (1989).
[18] F. Grossmann *et al.*, Phys. Rev. Lett. **67**, 516 (1991).
[19] J. Aumentado *et al.*, Phys. Rev. Lett. **92**, 066802 (2004).
[20] F. Bloch, Phys. Rev. **70**, 460 (1946).
[21] Yu. Makhlin, G. Schön, and A. Shnirman, cond-mat/0309049.
[22] The "ridges" connecting the maxima parallel to the gate offset axis arise as secondary interference maxima where $\tan(\varphi_L/2 - 2\tilde{\phi}_S)\cos\theta + \tan(\varphi_R/2 - 2\tilde{\phi}_S) = 0$. To obtain the ridges in Bloch simulations, we have to put $T_2 \gg T_1$, due to definition of the relaxation times in the instantaneous eigenbasis of the driven system.
[23] After submission of the present manuscript, a related, independent work on flux qubits appeared: W. D. Oliver *et al.*, Science **310**, 1653 (2005).
[24] M. A. Sillanpää, L. Roschier, and P. Hakonen, Phys. Rev. Lett. **93**, 066805 (2004).
[25] L. Roschier, M. Sillanpää, and P. Hakonen, Phys. Rev. B **71**, 024530 (2005).
[26] M. Sillanpää *et al.*, cond-mat/0510559.